Hydrology and Earth System Sciences

Discussions

Open Access

Climate change impacts on the seasonality and generation processes of floods in catchments with mixed snowmelt/rainfall regimes: projections and uncertainties

K. Vormoor[1], D. Lawrence[2], M. Heistermann[1], and A. Bronstert[1]

[1]Institute of Earth and Environmental Science, University of Potsdam, Karl-Liebknecht-Str. 24–25, 14476 Potsdam, Germany
[2]Norwegian Water Resources and Energy Directorate, Middelthunsgate 29, Postboks 5091 Majorstua, 0301 Oslo, Norway

Correspondence to: K. Vormoor (kvormoor@uni-potsdam.de)

Discussion Paper | Discussion Paper | Discussion Paper | Discussion Paper |

HESSD

11, 6273–6309, 2014

Climate change impacts on the seasonality and generation processes of floods

K. Vormoor et al.

Title Page

Abstract	Introduction
Conclusions	References
Tables	Figures

◄◄   ►►
◄   ►

Back   Close

Full Screen / Esc

Printer-friendly Version

Interactive Discussion

Abstract

Climate change is likely to impact the seasonality and generation processes of floods in the Nordic countries, which has direct implications for flood risk assessment, design flood estimation, and hydropower production management. Using a multi-model/multi-parameter approach, we analysed the projected changes in flood seasonality and its underlying generation processes in six catchments with mixed snowmelt/rainfall regimes in Norway. We found that autumn/winter events become more frequent in all catchments considered which leads to an intensification of the current autumn/winter flood regime for the coastal catchments, a reduction of the dominance of spring/summer flood regimes in a high-mountain catchment, and a possible systematic shift in the current flood regimes from spring/summer to autumn/winter in catchments in northern and south-eastern Norway. The changes in flood regimes results from increasing event magnitudes or frequencies, or a combination of both during autumn and winter. Changes towards more dominant autumn/winter events correspond to an increasing relevance of rainfall as a flood generating process (FGP) which is most pronounced in those catchments with the largest shifts in flood seasonality. Here, rainfall replaces snowmelt as the dominant FGP. We further analysed the ensemble components in contributing to overall uncertainty in the projected changes and found that the climate projections and the methods for downscaling or bias-correction tend to be the largest contributors. The relative role of hydrological parameter uncertainty, however, is highest for those catchments showing the largest changes in flood seasonality which confirms the lack of robustness in hydrological model parameterization for simulations under transient hydrometeorological conditions.

Title Page

Abstract | Introduction

Conclusions | References

Tables | Figures

◀◀ | ▶▶

◀ | ▶

Back | Close

Full Screen / Esc

Printer-friendly Version

Interactive Discussion

1 Introduction

The hydrological cycle is likely to intensify due to climate change (IPCC, 2007; Seneviratne et al., 2012), and a recent study indicates that global warming has caused more intense precipitation over the last century on the global scale (Benestad, 2013). These changes will, in turn, have direct implications for flood risk. A coherent picture of observed positive annual and winter streamflow trends for the Nordic countries (Stahl et al., 2010; Wilson et al., 2010) has been linked to a pattern of generally increasing mean and extreme precipitation (Bhend and von Storch, 2007; Dyrrdal et al., 2012). Climate projections for Norway until the end of the 21st century indicate increasing temperatures (2.3–4.6 °C) and precipitation (5–30 %) with the largest temperature increase during winter in northern Norway, and the largest precipitation increase during autumn and winter along the west coast (Hanssen-Bauer et al., 2009). Extreme precipitation is also likely to increase for all seasons across the whole of Norway (Beniston et al., 2007; Hanssen-Bauer et al., 2009; Seneviratne et al., 2012), although such projections are highly uncertain (Fowler and Ekström, 2009).

For the Nordic countries, several studies exist which investigate the hydrological impacts of climate change (e.g. Andréasson and Bergström 2004; Roald, 2006; Beldring et al., 2008; Veijalainen et al., 2010; Lawrence and Hisdal, 2011; Lawrence and Haddeland, 2011). For Norway, Lawrence and Hisdal (2011) studied the changes in flood frequency in 115 Norwegian catchments and found coherent regional patterns of directional change in flood frequency under a future climate: flood magnitudes are likely to increase in catchments in western and much of coastal Norway where flood generation is dominated by autumn/winter rainfall, while magnitudes are expected to decrease in the snowmelt-dominated catchments in inland areas and parts of northern Norway. This regional pattern reflects systematic changes in climate forcing which lead to changes in hydrological flooding in terms of both seasonal prevalence and generation process (rainfall vs. snowmelt). Considering the uncertainty in the projections for future (extreme) precipitation and subsequent flooding conditions (Bronstert et al.,

Full Screen / Esc

2007), Blöschl et al. (2011) argue that seasonal change in the distribution of floods is the key to understanding climate change impacts on flooding rather than changes in flood magnitudes and frequencies. Changes in the underlying flood generating processes (FGPs) are correspondingly important for interpreting the direction (i.e. increase vs. decrease) of climate change impacts on future floods.

For practical purposes, changes in flood seasonality have implications for future flood risk assessments, design flood estimations, and hydropower production management. In Norway, where hydropower represents about 96 % of the total electricity production, flood seasonality impacts reservoir management and accordingly hydropower production. In addition, design flood estimates for dam safety require that the season for the highest flood risk is assessed (e.g. Midttømme et al., 2011) and changes in the dominant flood season under a future climate have significant implications for these assessments. Despite the relevance of this issue, there has not yet been a detailed investigation of climate change impacts on future flood seasonality and the process-related factors contributing to those changes in Norway.

In this study, we investigate the impact of climate change on flood seasonality and the related FGPs in six Norwegian catchments representing different geographical and climatological conditions. The catchments were selected such that both rainfall and snowmelt sometimes play a role in the generation of high flow events under the current climate and we investigate how the balance between these two flood generating factors changes. We apply a multi-model/multi-parameter ensemble to derive a range of climate projection driven hydrological simulations which allows consideration of some of the uncertainties associated with the analysis. Our particular research questions are: (1) how might the existing regional patterns of flood seasonality change under a future climate? (2) How are shifts in seasonality related to changes in the magnitude vs. in the frequency of events? (3) Are changes in flood seasonality associated with changes in the dominant FGPs? (4) What is the relative importance of the different ensemble components in contributing to the overall variance as a measure of the uncertainty in the projected changes?

2 Study area

2.1 Climate and runoff regimes in Norway

Climatological gradients driven by latitude, topography and location relative to the coastal zone control the spatial pattern of temperature and precipitation regimes in Norway. The mean annual temperature varies from 7.7 °C at the south-western coast to about −3 °C in the inland areas of northern Norway and the high-altitude areas in central Norway (Hanssen-Bauer et al., 2009). Mean annual precipitation varies from about 300 mm in north-eastern and central Norway to more than 3500 mm in western Norway (Hanssen-Bauer et al., 2009). Seasonally, western Norway receives the highest precipitation amounts during autumn and winter while the more inland region in the east receives the highest amounts during summer.

Mean annual runoff generally reflects the pattern of mean annual precipitation and runoff coefficients tend to be high due to low evapotranspiration. However, due to differences in the temperature regime, snowpack volumes and the snow season vary considerably across the country, which leads to differences in the regional importance of snowmelt as a runoff generation process. Hence, two basic patterns in runoff regimes can be distinguished in Norway: (i) regions with prominent high flows during spring and summer predominantly due to snowmelt in inland and northernmost Norway, and (ii) regions with prominent high flows during autumn and winter predominantly due to rainfall in western Norway and in coastal regions. There are, though, numerous variations reflecting local climate, as well as transitional, mixed, regimes. In addition, catchments with sources in high mountain areas can experience peak flows in late summer, due to glacier melt. However, in order to develop a broad picture of flood seasonality, it is most useful to apply the simple distinction between rainfall and snowmelt as the most fundamental flood generation processes in Norway.

Title Page

Abstract | Introduction

Conclusions | References

Tables | Figures

◄ | ►

◄ | ►

Back | Close

Full Screen / Esc

Printer-friendly Version

Interactive Discussion

2.2 Study catchments

Changes in flood seasonality and the FGPs were investigated in six catchments distributed across Norway: Krinsvatn, Fustvatn, Øvrevatn, Junkerdalselv, Atnasjø, and Kråkfoss (Fig. 1). These catchments represent the climate variability and the basic hydrological regimes described above. The catchments are largely unaffected by damming or regulation (Petterson, 2004), and anthropogenic land use (changes) can be neglected since land use constitutes only between 0 and 1 % of land cover in all catchments excepting Kråkfoss (11 %). The catchments are included in the benchmark dataset for climate changes studies for Norway and are classified as suitable for daily analyses of flood discharge (Fleig et al., 2013). The six catchments are mesoscale catchments and vary in size from 207 km^2 (Krinsvatn) to 526 km^2 (Fustvatn). Further catchment characteristics including elevation, land cover, as well as mean annual precipitation and runoff are given in Table 1. Figure 1 displays flood roses to illustrate the magnitudes of the annual maximum floods (AMFs) from observed daily series by their Julian date of occurrence. These plots indicate the flood seasonality for the six catchments for the period indicated.

Although Krinsvatn and Fustvatn have the lowest elevations amongst the catchments, they receive a considerably higher annual precipitation (2291 and 3788 mm, respectively) due to their coastal locations. Correspondingly, the catchments have large average annual runoff values, and both the majority of and the largest AMFs occur during late autumn and winter, representing rainfall-dominated flood generation. However, both catchments are also subject to snowmelt floods, as indicated by the comparatively smaller events occurring during spring.

Øvrevatn, Junkerdalselv and Atnasjø show the highest mean elevation and elevation ranges, but differ considerably in annual precipitation and runoff volumes. Øvrevatn and Atnasjø, though being the highest catchments within this comparison, receive considerably less precipitation (832 and 840 mm, respectively) due to their rain shadow locations. Junkerdalselv, being located further inland near the Swedish border is not

immediately influenced by rain shadow effects and shows annual precipitation and runoff volumes that are about three times larger than at Øvrevatn and Atnasjø. Because of the temperature regime, all three catchments receive a large portion of the annual precipitation as snow so that the majority of and the largest AMFs occur during
5   spring and summer (May–July, Fig. 1), with snowmelt as the dominant FGP.

Kråkfoss, located inland of the Oslo fjord, is the southernmost catchment within this study and has a slightly different flood regime. There is no definite seasonal prevalence for the AMFs; one-half of the events occur during spring and summer, the other half during autumn and early winter. The magnitude of the autumn events tends to be slightly
10   larger than of those occurring during spring. Snowmelt plays a definite role in the early events in the spring/summer period; the events during autumn were triggered by rainfall. In addition, it is important to mention that for catchments dominated by snowmelt floods, the largest events almost always represent a combination of snowmelt and heavy rainfall. Similarly, most of the catchments dominated by rainfall-induced flood-
15   ing have periods in which a transient snowcover also may contribute to runoff during rainfall. Therefore, for this study it is useful to define a third FGP ("rainfall + snowmelt"), which occurs to varying degrees in all six catchments considered.

The dominant land cover types in the six catchments are either exposed (crystalline) bedrock with sparse vegetation above tree line (Atnasjø, 69 %; Junkerdalselv, 63 %;
20   Krinsvatn, 57 %; Øvrevatn, 57 %) or boreal forest (Kråkfoss, 76 %; Fustvatn, 38 %). Soils in all catchments are rather thin and poorly developed, and large, regional groundwater storage in aquifers is non-existent due to the crystalline bedrock. However, in most catchments, surface water in the form of lakes, marshes and bogs leads to water retention and, in some cases, attenuation of flood peaks.

3   Data and methods

3.1   Modeling strategy

The analyses of changes in flood seasonality and their associated FGPs are based on a multi-model/multi-parameter ensemble approach consisting of (i) eight GCM/RCM combinations, (ii) two methods for adjusting the temperature and precipitation outputs of the climate models at the catchments scale, and (iii) the HBV hydrological model with 25 different parameter sets for considering hydrological parameter uncertainty and equifinality. The following subsections describe the individual components of the ensemble in more detail.

3.2   Climate projections

The climate projections for precipitation and temperature chosen for the hydrological simulations are based on eight GCM/RCM combinations (Table 2) from the EU FP6 ENSEMBLES project (van der Linden and Mitchell, 2009). The spatial resolution of all RCMs considered is 0.22° (approximately 25 km), and projections of daily values are available for the period 1950–2100 or 1950–2099. Within this study, two periods are compared: a reference period (1961–1990) for which the GCM/RCM combinations are driven by the IPCC-AR4 scenario C20, and a future period (2071–2099) for which the climate model combinations are driven by the SRES A1B scenario, which represents intermediate greenhouse gas emissions until the end of the 21st century (IPCC, 2000, 2007). We selected the eight RCMs from ENSEMBLES that are nested into as many different GCMs as possible to minimize interdependency between the climate model outputs used (Sunyer et al., 2013).

3.3   Local Adjustment Methods (LAMs)

It is widely acknowledged that the RCM outputs for the variables of interest (in our case precipitation and temperature) are biased due to limited process description, biased

fluxes at the RCM margins and insufficient spatial resolution relative to the catchment scale (Engen-Skaugen et al., 2007). Therefore, data post-processing is necessary to bridge the gap between the large-scale climate model and the local hydrological processes (e.g. Maraun et al., 2010; Chen et al., 2011). Considerable progress has been made during recent years regarding the development and improvement of such methods and Hanssen-Bauer et al. (2005), Fowler et al. (2007), Maraun et al. (2010), and Teutschbein and Seibert (2012) give comprehensive reviews on available approaches.

Amongst the LAMs, a useful distinction can be made between statistical downscaling and bias correction methods. In this study two different LAMs were applied: (i) Empirical Quantile Mapping (Boé et al., 2007; Gudmundsson et al., 2012) representing a bias correction method, and (ii) Expanded Downscaling (Bürger, 1996; Bürger et al., 2009) which is a type of statistical downscaling.

3.3.1 Empirical Quantile Mapping (EQM)

EQM is a bias correction method that seeks a transfer function (h) to adjust RCM data so that it is in better agreement with observations. By adjusting the quantiles of the biased RCMs (x_m) to those of the locally observed data (x_o), the bias-corrected distribution of x_m should match the distribution of x_o, such that:

$$x_o = h(x_m) = F_o^{-1}(F_m(x_m)) \tag{1}$$

where F_m is the empirical cumulative distribution function (eCDF) of x_m, and F_o^{-1} is the inverse eCDF (the quantile function) corresponding to x_o. Based on the assumption that the shortcomings of the climate model are the same for the reference and future periods (van Roosmalen et al., 2011) and that the transfer function is stationary in time (Maraun et al., 2010), the function is applied to bias correct projections from RCMs for both the reference and future period.

For Norway, Gudmundsson et al. (2012) found that non-parametric transfer methods (as EQM) performed best for the bias correction of precipitation compared to

parametric and distribution derived transformations. Therefore EQM was considered as a suitable LAM for the correction of daily precipitation and temperature values for this study. The method was implemented as an add-on package ("qmap", Gudmundsson, 2012) for the statistical programming environment R (R Core Team, 2012). Bias correction was performed on daily values for the full year, without distinguishing seasons, following work of Piani et al. (2009) which illustrated that this approach performs remarkably well.

3.3.2 Expanded Downscaling (XDS)

XDS is a statistical downscaling approach, and as such it maps large-scale atmospheric fields (the predictors (x)) to local data (the predictands (y)). XDS has been applied for various purposes, e.g. for early flood warning (Bürger et al., 2009), downscaling extreme precipitation projections (Dobler et al., 2013), and hydrological impact studies (Dobler et al., 2012a).

At its core, XDS is based on multiple linear regression (MLR) which leads to minimizing the least square errors. The drawback of MLR, however, is that local climate variability will be smoothed significantly which has strong implications for the simulation of extremes. To overcome this limitation, XDS adds an additional condition for retaining local co-variability between the variables:

$$XDS = \arg\min_{Q} \|x\mathbf{Q} - y\|, \quad \text{subjected to } \mathbf{Q}'x'x\mathbf{Q} = y'y, \tag{2}$$

such that XDS is the solution of the error-minimizing matrix $\mathbf{Q}(x\mathbf{Q} - y)$ which is found amongst those that preserve the local covariance ($\mathbf{Q}'x'x\mathbf{Q} = y'y$). This approach is supposed to improve the estimation of extreme events, at the cost of a larger mean error as compared to conventional MLR.

For the present study, we used humidity, wind fields, temperature, and precipitation characteristics as predictor fields. XDS was calibrated on the RCM atmospheric fields driven by the ECMWF ERA-40 reanalysis (Uppala et al., 2005) for the period

1961–1980, and then applied to downscale the RCM outputs for the reference and future scenarios.

3.4 The HBV model

The analysis of climate change impacts at the catchment scale is based on daily
streamflow simulated by the lumped, conceptual HBV model (Bergström 1976, 1995), forced by the locally adjusted RCM data. In this study we apply the "Nordic" version of the model (Sælthun, 1996), which incorporates a snow module with equal area height zones, such that snow accumulation and melting has a semi-distributed structure. The principal advantage of the HBV model relative to more physically-based models are
that it only requires precipitation and temperature as climatological input.

The HBV model was calibrated for each catchment using daily-averaged discharge data. Excepting Kråkfoss, where observed data are only available since 1966, the entire reference period (1961–1990) was used for model calibration. The model calibration uses the Dynamically Dimensioned Search (Tolson and Shoemaker, 2007) (DDS)
which is a global optimization algorithm for the calibration of multi-parameter models. A modified version of the Nash–Sutcliffe efficiency (NSE_w) was used as the objective function so as to focus on matching the high flow events:

$$NSE_w = 1 - \frac{\sum_{i=1}^{n} Q_{obs}(Q_{sim} - Q_{obs})^2}{\sum_{i=1}^{n} Q_{obs}(Q_{sim} - \overline{Q_{obs}})^2} \qquad (3)$$

where Q_{obs} represents the observed discharges and Q_{sim} represent the modeled discharges. The squared differences in the numerator and denominator are weighted by the observed discharge. A mismatch between high observed and simulated discharges is, therefore, penalized proportionally to the observed discharge value.

To account for parameter uncertainty and equifinality, 25 best-fit parameter sets were
identified and included for the hydrological simulations. Fifteen free parameters were subjected to the calibration by DDS, which was setup to 1200 model calls. The best

performing parameter set was taken directly from the DDS calibration. The remaining 24 parameter sets were identified by a subsequent Monte-Carlo simulation with another 1200 model calls using a narrowed range in the parameter values which was defined by the range of parameter values of the 36 (= 3 %) best parameter sets identified by DDS. In that way, effects of interdependency between the parameter sets is minimized.

3.5 Change analysis

The extreme events of the daily streamflow simulations were extracted using a Peak Over Threshold (POT) approach, which leads to a more comprehensive selection of events (in terms of timing and flood processes) compared the Block Maximum method (i.e. AMF) (Lang et al., 1999). The threshold was set to the 98.5 streamflow percentile. Independency of events was achieved by enforcing that (i) only one event can occur within twice the normal flood duration (which is catchment specific) and (ii) that only the largest event will be considered if more than one peak is identified within that time period.

3.5.1 Changes in flood seasonality

Detected POT events were divided into two seasons reflecting the basic flood regimes described in Sect. 2.1: (i) the spring/summer period from March to August which is currently associated with snowmelt as an important FGP, and (ii) the autumn/winter period from September to February which is associated with rainfall as the most important FGP. To quantify the seasonality of flood events, we suggest a seasonality index S_D:

$$S_D = \frac{POT_{sep\text{-}feb}}{POT_{all}} - \frac{POT_{mar\text{-}aug}}{POT_{all}} \qquad (4)$$

where the first term describes the ratio between the flood peaks [$m^3 s^{-1}$] of the POT events occurring within the period September to February over all POT events, and the second term describes the ratio between the POT events occurring within March to

Printer-friendly Version

Interactive Discussion

August over all POT events. The index ranges from −1 to +1: negative numbers indicate dominant events during spring/summer while positive numbers indicate dominant events during autumn/winter. S_D was estimated for each ensemble member for both the reference and the future periods. The difference in S_D between the future and the reference period is an indicator for changes in flood seasonality.

3.5.2 Changes in FGPs

Each POT event was analyzed regarding the dominant contribution to flood discharge. This contribution has been inferred from the runoff components simulated by the HBV model. A simple water balance approach was used to classify the events into floods generated by (i) "rainfall", (ii) "rainfall + snowmelt" and (iii) "snowmelt". The classification is based on the relative contribution of the volumes of rainfall and snowmelt to the flood event discharge: an event was classified as "rainfall" if the contribution of rainfall was larger than 2/3, and classified as "snowmelt" if rainfall contribution was smaller than 1/3. Other events were classified as "rainfall + snowmelt".

In order to also account for the antecedent conditions in the catchment, the flood duration time of the core event was extended by adding the catchment specific recession time before the onset of the core flood. The classification approach was then applied to the extended flood duration time. The ratios of rainfall-, rainfall + snowmelt- and snowmelt-generated events relative to all events for all ensemble realizations were estimated for the reference and future period. The change in the ratios indicates the changes in the prevalence of the different FGPs.

3.6 Sources of uncertainty

The range of all ensemble realizations provides a measure of the overall uncertainty represented by the ensemble, given that each projection is assumed to be equally likely. Similar to Déqué et al. (2007, 2011), the mean variance $\overline{\sigma^2}_{\text{ensemble}}$ (as a measure of

uncertainty) of the entire ensemble is here defined as the additive mean variances from the ensemble components:

$$\overline{\sigma^2}_{ensemble} = \overline{\sigma^2}_{GCM/RCM} + \overline{\sigma^2}_{LAM} + \overline{\sigma^2}_{HP}. \tag{5}$$

5 We exemplify the computation of mean variances from the ensemble components for the hydrological model parameterization ($\overline{\sigma^2}_{HP}$): for each combination i out of n possible combinations of GCM/RCMs and LAMs, we compute the variance $\sigma_{HP,i}$ subject to 25 parameter sets of the hydrological model. Then, we compute $\overline{\sigma^2}_{HP}$ as the mean over all $\sigma_{HP,i...n}$. $\overline{\sigma^2}_{GCM/RCM}$ and $\overline{\sigma^2}_{LAM}$ are computed accordingly.

10   This approach was used to identify the fractional uncertainty emerging from the different sources within the model chain for three variables: (i) the change in the index S_D, (ii) the change in the median magnitude of the POT events, and (iii) the change in the fraction of snowmelt- over rainfall-generated events.

4   Results and discussion

15 ### 4.1   Model and ensemble validation

The performance of the HBV model is validated using the 25 best-fit parameter sets to estimate POT events during the reference period. These are compared to the distribution of observed POT events for the same period. In this case, the HBV simulations are based on observed meteorological data. Furthermore, we evaluated the ability of
20 the entire ensemble (i.e. including all GCM/RCM combinations, LAMs, and hydrological parameter sets) to match the observed POT events for the reference period. A further comparison was made with HBV simulations based on the raw RCM data and the adjusted RCM data to assess the potential benefit of the adjustment procedures. The distribution of the POT events for each of these options is illustrated in Fig. 2.

The results indicate that the HBV model using the 25 best-fit parameter sets with observed climate data reproduces the observed POT events reasonably well for almost all of the catchments. For Junkerdalselv, the mismatch between the distribution of observed vs. simulated POT events is considerably larger than in other catchments. Junkerdalselv also has the lowest NSE_w value (0.77). The NSE_w value for the other five catchments varies from 0.83 (Fustvatn) to 0.91 (Atnasjø).

As expected, the absolute range and the interquartile range of the POT event distribution from the full ensemble are larger. However, in four catchments the quartiles match the observed distribution fairly well (Krinsvatn, Øvrevatn, Atnasjø, Kråkfoss). The largest discrepancies occur for Fustvatn and Junkerdalselv. In both cases, the mismatch of the ensemble reflects the overestimation (Fustvatn) and underestimation (Junkerdalselv) resulting from the different LAMs. The performance of the ensemble in reproducing the observed POT events is the only indicator we have of how reliable the ensemble is for future projections. For Fustvatn and Junkerdalselv, that implies a smaller reliability of the future projections compared to the remaining catchments.

Figure 2 also underlines the benefit of locally adjusting raw RCM data for hydrological simulations. The large ranges in the distribution of the simulations based on RCM raw data are narrowed considerably after adjustment at Øvrevatn, Junkerdalselv, Atnasjø and Kråkfoss by both LAMs. Moreover, the LAMs are able to correct the large discrepancies in the POT event distributions for the observed vs. the simulated series for Krinsvatn, Fustvatn and Atnasjø. For Fustvatn, the benefit of the local adjustment is least since the underestimation of the RCM raw data is only corrected to an overestimation of almost the same magnitude and range. It is not possible to conclude which of the two LAMs is better suited for high flow estimations, neither in general nor for specific geographical regions.

4.2 Changes in flood seasonality

Figure 3 summarizes the results for the index S_D for the reference and future period for the six study catchments. The boxplots represent the full ensemble.

For the reference period, the S_D quartiles for the west coast catchments Krinsvatn and Fustvatn show positive values which indicate dominant autumn/winter POT events. For Øvrevatn and Junkerdalselv in the north, as well as for Atnasjø and Kråkfoss in central and south-eastern Norway, the S_D quartiles indicate dominant POT events during spring/summer. The dominance of spring/summer events is largest for Atnasjø, but Junkerdalselv also shows a distinct spring/summer pattern with negative S_D values for all ensemble realizations. For Kråkfoss, this dominance is least pronounce. The observed flood seasonality (indicated by the green bars) is matched reasonably well in five of the six catchments (Krinsvatn, Fustvant, Øvrevatn, Junkerdalselv, Atnasjø), with Fustvatn and Øvrevatn having the best matches. For Kråkfoss, however, the S_D values for the majority of the ensemble realizations are rather low suggesting that the dominance of spring/summer events is overestimated to some degree by the model simulations.

For the future period, the S_D values are higher for all catchments. That means that the importance of autumn/winter events is projected to increase in all catchments considered. The lowest impact is found for Atnasjø where the dominance of spring/summer events persists into the future. However, for Øvrevatn and Kråkfoss considerably higher S_D values indicate a possible seasonal shift in the flood regimes since S_D becomes positive for almost the entire interquartile of all ensemble realizations. Changes towards dominant autumn/winter events are also indicated by some ensemble members for Junkerdalselv. However, the first and second quartiles still show negative S_D values.

The ranges in the projections given by the boxplots indicate the uncertainty associated with the ensemble. For the reference period, this is highest for Fustvatn and Kråkfoss. For the future period, the highest ranges are found for Øvrevatn, Junkerdalselv and Kråkfoss which are showing the largest change in flood seasonality. Note that the projected changes in seasonality are significant for all regions since the notches of the boxplots for the reference and future periods are not overlapping in any of the catchments.

4.3 Changes in the magnitude vs. the frequency of events

After having detected changes in flood seasonality, the question arises as to whether these result from changes in flood magnitude vs. frequency in the two respective seasons. Figure 4 summarizes the POT events for all ensemble realizations according to their associated magnitudes and number of occurrences for the two seasons.

For the coastal catchments, Krinsvatn and Fustvatn, Fig. 4 shows that both the number and the magnitude of POT events increase in autumn/winter. For spring/summer, the magnitude also increases, but the frequency decreases (i.e. the blue boxes show smaller widths). Together, this explains the intensification of the seasonality index S_D towards autumn/winter events. The seasonal shift towards autumn/winter events is even more pronounced for the northernmost catchments, Øvrevatn and Junkerdalselv (Fig. 3). Figure 4 indicates that this shift is mostly due to changes in the frequency (increasing in autumn/winter, decreasing in spring/summer) while the mean magnitudes are decreasing in both seasons. Note, however, that the observed seasonal POT magnitudes are not well reproduced by the ensemble for Junkerdalselv. For the high-altitude catchment in central Norway, Atnasjø, Fig. 3 indicates that spring/summer events are very dominant in both the current and future climate. Figure 4 establishes that this dominance reflects the frequency of the events in the POT series, and not necessarily the magnitude. Future flood magnitudes increase slightly for both seasons, while frequencies increase particularly in autumn/winter period. This is responsible for the slight shift in seasonal index in Fig. 3. Finally, Fig. 4 also illustrates that the large seasonal shift for Kråkfoss is caused by both frequencies (decrease in spring/summer, increase in autumn/winter) and magnitudes. Future flood magnitudes increase in both seasons, but the increase in autumn/winter is considerably larger.

Note that the discrepancies between the observed and simulated POT magnitudes for the reference period (i.e. Fig. 2) are also reflected in the seasonal values in Fig. 4. The large discrepancy at Junkerdalselv and Atnasjø for the autumn/winter period is due to the limited number of observed events during these months.

4.4 Changes in FGPs

In the previous sections, we established that autumn/winter events will become more dominant in the future. This is consistent over all investigated catchments, although there are differences with respect to their underlying causes (i.e. changes in frequency, magnitude, or both). In general, we would expect that an increasing dominance of autumn/winter events corresponds to an increasing importance of rainfall as a FGP. Figure 5 shows how the percentage of different flood generating processes will change from the reference to the future period:

Rainfall becomes the dominant FGP in the future period in all investigated catchments. For the coastal catchments, Krinsvatn and Fustvatn, where rainfall already dominates flood generation before, it will become even more important in the future. Snowmelt generated floods, which plays only a minor role here during the reference period, will vanish completely. In the remaining four catchments, rainfall replaces snowmelt as the dominant FGP. The highest increase in the importance of rainfall is projected for the northernmost catchments, Øvrevatn and Junkerdalselv, and the south-eastern catchment, Kråkfoss, where the changes in flood seasonality are also highest. This proves that changes in flood seasonality are closely connected to changes in the FGPs.

Further changes of the FGPs are connected with an earlier timing and decreasing magnitudes of the POT events associated with snowmelt in catchments where this FGP continues to be relevant. Moreover, rainfall-generated POT events tend to occur later within the year across all catchments. Figure 6 illustrates the relationship between changes in the FGPs and the median magnitude of the events as a function of their circular mean Julian date of occurrence.

Higher mean temperatures lead to an earlier onset of the annual snowmelt season. For the catchments which continue to have peak discharges associated with snowmelt in the future period, the circular mean Julian dates of occurrence of the snowmelt-generated events is estimated to be 14–26 days earlier compared to the reference

Title Page

Abstract | Introduction

Conclusions | References

Tables | Figures

◄ | ►

◄ | ►

Back | Close

Full Screen / Esc

Printer-friendly Version

Interactive Discussion

period: Øvrevatn (26 days), Junkerdalselv (21days), Atnasjø (14 days), Kråkfoss (22 days). This agrees with similar findings from streamflow observations and projections for the Nordic countries (Beldring et al., 2008; Stahl et al., 2010; Wilson et al., 2010) and for other parts in the world (Stewart et al., 2005; Déry et al., 2009; Renner and Bernhofer, 2011; Kormann et al., 2014). With the exception of Kråkfoss, the mean magnitude of the POT events generated by snowmelt will decrease in all catchments where snowmelt has an influence on flooding in the future period. This is because of smaller snowpack volumes due to shorter and warmer winters in the future period (Vikhamar Schuler et al., 2006).

The increasing POT event magnitudes during autumn and winter at Fustvatn, Atnasjø and Kråkfoss (Fig. 4) can be explained by the increasing mean magnitudes of rainfall generated events in those catchments (Fig. 6). The increasing magnitudes of autumn/winter events at Krinsvatn (Fig. 4) result from an earlier circular mean timing of the rainfall+snowmelt events in the future period (from March to February; Fig. 6). The circular density functions show that rainfall has an influence on flooding throughout the year particularly during autumn and winter for both the reference and future period. Prominent seasonal peaks of rainfall generated POT events during the reference period, as they are observed for Kråkfoss (October–November), will be smoothed in the future period. Thus, rainfall becomes more relevant for spring and summer, as well as winter events in the future period. The later mean timing of rainfall generated events for all catchments highlights the increasing importance of winter rainfall floods for the future period. For Øvrevatn, Junkerdalselv and Kråkfoss, this suggests that winter precipitation is no longer principally received as snowfall so that the contribution of snowmelt to runoff is considerably less in the future period. Thus, the strongest changes in flood seasonality are observed for these catchments which is in line with Arnell (1999) who concludes that the most significant changes in flow regimes occur where snowfall becomes less important due to higher temperatures.

4.5 Contribution of ensemble components to uncertainty

Figure 7 shows the fractional variance from the different sources of the ensemble as they contribute to the total variance regarding the changes in the index S_D, the POT magnitudes and the FGPs presented in Figs. 3–6.

First of all, the GCM/RCM combinations and the LAMs are the dominant sources of uncertainty for all catchments and variables considered. Hydrological model parameterization tends to be the smallest contributor to overall uncertainty, which is in line with earlier studies (e.g. Wilby and Harris, 2006; Kay et al., 2008; Prudhomme and Davies, 2008; Dobler et al., 2012b). Note, however, that there are exceptions where the variance due to the hydrological model parameterization is as high as that due to the LAMs or the climate projections (i.e. Junkerdalselv, 2nd and 3rd column). Focusing on the target variables, hydrological parameter uncertainty tends to be less important for changes in the seasonality index S_D as compared with changes in the POT event magnitudes and the dominant FGPs.

A possible regional pattern becomes apparent regarding the relative role of hydrological parameter uncertainty which seems to be closely connected to the changes in flood seasonality and FGPs. Hydrological parameter uncertainty is rather high in those catchments for which a considerable change in their flood seasonality and the FGPs is expected (Øvrevatn, Junkerdalselv, Kråkfoss). This is probably due to changes in the dominant flood generation mechanisms. It is likely that the parameter sets which are calibrated for the climate conditions in the reference period are not sufficiently stable given the likely changes in hydroclimatological- and runoff generation processes under future conditions. This highlights the difficulties associated with transferring model parameters in time under non-stationary conditions (Merz et al., 2011; Brigode et al., 2013). It further stresses the need for alternative calibration approaches which improve the robustness of the hydrological model simulations such that they are able to adapt changes in the dominant runoff generation mechanisms under future conditions.

5 Conclusions

Using a multi-model/multi-parameter ensemble approach, the impacts of climate change on flood seasonality and their underlying flood generating processes (FGPs) in different regions in Norway have been investigated.

The results indicate that the HBV model, including the use of 25 best-fit parameter sets, is able to reproduce observed distributions of flood events reasonably well for five out of six study catchments for the reference period. Small discrepancies between the event distributions simulated by the locally-adjusted climate projection data and the observed event distributions slightly reduce the reliability of the ensemble setup for two catchments (Fustvatn, Junkerdalselv). For the remaining four catchments the ensemble reproduces the observed flood event distributions fairly well. The benefit of post-processing the RCM raw data has also been demonstrated. However, no distinct ranking emerged regarding the performance of the two LAMs applied.

Reconsidering our research questions, the following conclusions can be drawn:

– *How might the existing patterns of flood seasonality change under a future climate?*
   Autumn/winter floods become more important in all the catchments considered. For the coastal catchments that suggests an intensification of the current autumn/winter flood regime. For the high-mountain catchment, Atnasjø, in central Norway, the dominance of spring/summer flood will be slightly reduced. For the northernmost catchments, Øvrevatn and Junkerdalselv, as well as for the southeastern catchment, Kråkfoss, the increase in autumn/winter floods is largest and may lead to a systematical shift in the current flood regimes from spring/summer to autumn/winter.

– *How are the shifts in seasonality related to changes in the magnitude vs. in the frequency of events?*
   Changes in flood seasonality from spring/summer towards autumn/winter are the result of increasing event magnitudes or frequencies, or a combination of both,

during the autumn and winter months. Changes in seasonal frequency, however, are more relevant than changes in seasonal magnitude since two of the catchments with the strongest changes in flood seasonality (Øvrevatn and Junkerdalselv) show decreasing flood magnitudes but large shifts in the seasonal frequency of events.

- *Are changes in flood seasonality associated with changes in the FGPs?*
  The change towards more autumn/winter events corresponds to an increasing relevance of rainfall as a FGP. Rainfall becomes more dominant where it already has been dominant before, and it replaces snowmelt as the dominant FGP in the remaining catchments. The largest increases in the relative role of rainfall correspond with the largest shifts in flood seasonality (Øvrevatn, Junkerdalselv, Kråkfoss). In these catchments, less snow accumulation and shorter snow seasons due to increased winter temperatures lead to a considerable decrease in the frequency and magnitude of snowmelt-generated events. Additionally, rainfall-generated events occur more often and also later within the autumn/winter period. Thus, the largest changes in the FGPs are closely connected with temperature effects which determine the relative role of snowmelt vs. rainfall. This has a major influence on the seasonal distribution of floods.

- *What is the relative importance of the different ensemble components in contributing to the overall variance as a measure of the uncertainty in the projected changes?*
  For changes in flood seasonality the ensemble range is largest in those catchments for which the largest seasonal changes are projected. The climate projections (i.e. the GCM/RCM combinations) or the LAMs tend to be the largest contributor to the total variance. However, the relative role of the hydrological model parameterization compared to both other contributors is highest for those catchments showing the most pronounced seasonal changes. This is consistent with an earlier study of climate change impacts in four Norwegian catchments (Lawrence

and Haddeland, 2011), and confirms the lack of robustness in HBV parameterizations for simulations with transient hydrometeorological conditions which lead to changes in the flood regime.

References

Andréasson, J. and Bergström, S.: Hydrological change-climate change impact simulations for Sweden, Ambio, 33, 228–234, 2004.

Arnell, N. W.: The effect of climate change on hydrological regimes in Europe: a continental perspective, Global Environ. Change, 9, 5–23, 1999.

Beldring, S., Engen-Skaugen, T., Førland, E. J., and Roald, L. A.: Climate change impacts on hydrological processes in Norway based on two methods for transferring regional climate model results to meteorological station sites, Tellus A, 60, 439–450, doi:10.1111/j.1600-0870.2008.00306.x, 2008.

Benestad, R. E.: Association between trends in daily rainfall percentiles and the global mean temperature, J. Geophys. Res.-Atmos., 118, 10802–10810, doi:10.1002/jgrd.50814, 2013.

Beniston, M., Stephenson, D. B., Christensen, O. B., Ferro, C. A. T., Frei, C., Goyette, S., and Woth, K.: Future extreme events in European climate: an exploration of regional climate model projections, Climatic Change, 81, 71–95, doi:10.1007/s10584-006-9226-z, 2007.

Bergström, S.: Development and Application of a Conceptual Runoff Model for Scandinavian Catchments, SMHI Reports RHO, No. 7, SMHI, Nörrköping, 1976.

Bergström, S.: The HBV model, in: Computer Models of Watershed Hydrology, Water Resources Publications, Highlands Ranch, CO, 443–476, 1995.

Bhend, J. and von Storch, H.: Consistency of observed winter precipitation trends in northern Europe with regional climate change projections, Clim. Dynam., 31, 17–28, doi:10.1007/s00382-007-0335-9, 2007.

Title Page

Abstract | Introduction

Conclusions | References

Tables | Figures

◄ | ►

◄ | ►

Back | Close

Full Screen / Esc

Printer-friendly Version

Interactive Discussion

Blöschl, G., Viglione, A., Merz, R., Parajka, J., Salinas, J. L., and Schöner, W.: Auswirkungen des Klimawandels auf Hochwasser und Niederwasser, Österreichische Wasser- und Abfallwirtschaft, 63, 21–30, doi:10.1007/s00506-010-0269-z, 2011.

Boé, J., Terray, L., Habets, F., and Martin, E.: Statistical and dynamical downscaling of the Seine basin climate for hydro-meteorological studies, Int. J. Climatol., 27, 1643–1655, doi:10.1002/joc.1602, 2007.

Brigode, P., Oudin, L., and Perrin, C.: Hydrological model parameter instability: a source of additional uncertainty in estimating the hydrological impacts of climate change?, J. Hydrol., 476, 410–425, doi:10.1016/j.jhydrol.2012.11.012, 2013.

Bronstert, A., Kolokotronis, V., Schwandt, D., and Straub, H.: Comparison and evaluation of regional climate scenarios for hydrological impact analysis: general scheme and application example, 1594, 1579–1594, doi:10.1002/joc.1621, 2007.

Bürger, G.: Expanded downscaling for generating local weather scenarios, Clim. Res., 7, 111–128, doi:10.3354/cr007111, 1996.

Bürger, G., Reusser, D., and Kneis, D.: Early flood warnings from empirical (expanded) downscaling of the full ECMWF Ensemble Prediction System, Water Resour. Res., 45, W10443, doi:10.1029/2009WR007779, 2009.

Chen, J., Brissette, F. P., and Leconte, R.: Uncertainty of downscaling method in quantifying the impact of climate change on hydrology, J. Hydrol., 401, 190–202, doi:10.1016/j.jhydrol.2011.02.020, 2011.

Déqué, M., Rowell, D. P., Lüthi, D., Giorgi, F., Christensen, J. H., Rockel, B., Jacob, D., Kjellström, E., Castro, M., and Hurk, B.: An intercomparison of regional climate simulations for Europe: assessing uncertainties in model projections, Climatic Change, 81, 53–70, doi:10.1007/s10584-006-9228-x, 2007.

Déqué, M., Somot, S., Sanchez-Gomez, E., Goodess, C. M., Jacob, D., Lenderink, G., and Christensen, O. B.: The spread amongst ENSEMBLES regional scenarios: regional climate models, driving general circulation models and interannual variability, Clim. Dynam., 38, 951–964, doi:10.1007/s00382-011-1053-x, 2011.

Déry, S. J., Stahl, K., Moore, R. D., Whitfield, P. H., Menounos, B., and Burford, J. E.: Detection of runoff timing changes in pluvial, nival, and glacial rivers of western Canada, Water Resour. Res., 45, W04426, doi:10.1029/2008WR006975, 2009.

Climate change impacts on the seasonality and generation processes of floods

K. Vormoor et al.

Title Page

Abstract	Introduction
Conclusions	References
Tables	Figures

◄ | ►|

◄ | ►

Back | Close

Full Screen / Esc

Printer-friendly Version

Interactive Discussion

Dobler, C., Bürger, G., and Stötter, J.: Assessment of climate change impacts on flood hazard potential in the Alpine Lech watershed, J. Hydrol., 460–461, 29–39, doi:10.1016/j.jhydrol.2012.06.027, 2012a.

Dobler, C., Hagemann, S., Wilby, R. L., and Stötter, J.: Quantifying different sources of uncertainty in hydrological projections in an Alpine watershed, Hydrol. Earth Syst. Sci., 16, 4343–4360, doi:10.5194/hess-16-4343-2012, 2012b.

Dobler, C., Bürger, G., and Stötter, J.: Simulating future precipitation extremes in a complex Alpine catchment, Nat. Hazards Earth Syst. Sci., 13, 263–277, doi:10.5194/nhess-13-263-2013, 2013.

Dyrrdal, A., Isaksen, K., Hygen, H., and Meyer, N.: Changes in meteorological variables that can trigger natural hazards in Norway, Clim. Res., 55, 153–165, doi:10.3354/cr01125, 2012.

Engen-Skaugen, T., Haugen, J. E., and Tveito, O. E.: Temperature scenarios for Norway: from regional to local scale, Clim. Dynam., 29, 441–453, doi:10.1007/s00382-007-0241-1, 2007.

Fleig, A. K., Andreassen, L. M., Barfod, E., Haga, J., Haugen, L. E., Hisdal, H., Melvold, K., and Saloranta, T.: Norwegian Hydrological Reference Dataset for Climate Change Studies, Norwegian Water Resources and Energy Directorate (NVE), Oslo, 2013.

Fowler, H. J. and Ekström, M.: Multi-model ensemble estimates of climate change impacts on UK seasonal precipitation extremes, Int. J. Climatol., 29, 385–416, doi:10.1002/joc.1827, 2009.

Fowler, H. J., Blenkinsop, S., and Tebaldi, C.: Linking climate change modelling to impacts studies: recent advances in downscaling techniques for hydrological modelling, Int. J. Climatol., 27, 1547–1578, doi:10.1002/joc.1556, 2007.

Gudmundsson, L., Bremnes, J. B., Haugen, J. E., and Engen-Skaugen, T.: Technical Note: Downscaling RCM precipitation to the station scale using statistical transformations – a comparison of methods, Hydrol. Earth Syst. Sci., 16, 3383–3390, doi:10.5194/hess-16-3383-2012, 2012.

Hanssen-Bauer, I., Achberger, C., Benestad, R. E., Chen, D., and Førland, E. J.: Statistical downscaling of climate scenarios over Scandinavia, Clim. Res., 29, 255–268, 2005.

Hanssen-Bauer, I., Drange, H., Førland, E., Roald, L. A., Børsheim, K. Y., Hisdal, H., Lawrence, D., Nesje, A., Sandven, S., Sorteberg, A., Sndby, S., Vasskog, K. and Ådlandsvik, B.: Klima i Norge 2100 Bakgrunnsmateriale til NOU Klimatilpasning (Climate in Norway 2100 background material for NOU climate adaptation), Norsk klimasenter, Oslo., 2009.

IPCC: Special Report on Emission Scenarios – Summary for Policymakers, Cambridge University Press, Cambridge, UK, 2000.

IPCC: Climate Change 2007: The Physical Science Basis, edited by: Solomon, S., Qin, D., Manning, M., Chen, Z., Marquis, M., Averyt, K. B., Tignor, M., and Miller, H. L., Cambridge University Press, Cambridge, UK, and New York, NY, USA, 2007.

Kay, A. L., Davies, H. N., Bell, V. A., and Jones, R. G.: Comparison of uncertainty sources for climate change impacts: flood frequency in England, Climatic Change, 92, 41–63, doi:10.1007/s10584-008-9471-4, 2008.

Kormann, C., Francke, T., and Bronstert, A.: Daily-resolution trend analysis applied to Alpine hydro-climatic station data in Tyrol, Autria, J. Water Clim. Change, in review, 2014.

Lang, M., Ouarda, T. B. M. J., and Bobée, B.: Towards operational guidelines for over-threshold modeling, J. Hydrol., 225, 103–117, doi:10.1016/S0022-1694(99)00167-5, 1999.

Lawrence, D. and Haddeland, I.: Uncertainty in hydrological modelling of climate change impacts in four Norwegian catchments, Hydrol. Res., 42, 457, doi:10.2166/nh.2011.010, 2011.

Lawrence, D. and Hisdal, H.: Hydrological Projections for Floods in Norway under a Future Climate, Report 5-2011, Norwegian Water Resources and Energy Directorate, Oslo, 2011.

Maraun, D., Wetterhall, F., Ireson, A., Chandler, R., Kendon, E., Widmann, M., and Thiele-Eich, I.: Precipitation downscaling under climate change: recent developments to bridge the gap between dynamical models and the end user, Rev. Geophys., 48, 1–34, 2010.

Merz, R., Parajka, J., and Blöschl, G.: Time stability of catchment model parameters: implications for climate impact analyses, Water Resour. Res., 47, W02531, doi:10.1029/2010WR009505, 2011.

Midttømme, G. H., Petterson, L. E., Holmqvist, E., Nøtsund, Ø., Hisdal, H., and Sivertsgård, R.: Retningslinjer for flomberegninger ("Guidelines for Flood Estimation"), NVE retningslinjer 4/2011, Oslo, 2011.

Petterson, L. E.: Aktive vannføringsstasjoner i Norge ("Active Streamflow Gauges in Norway"), NVE Rapport 16/2004, Oslo, 2004.

Piani, C., Haerter, J. O., and Coppola, E.: Statistical bias correction for daily precipitation in regional climate models over Europe, Theor. Appl. Climatol., 99, 187–192, doi:10.1007/s00704-009-0134-9, 2009.

Prudhomme, C. and Davies, H.: Assessing uncertainties in climate change impact analyses on the river flow regimes in the U K, Part 2: future climate, Climatic Change, 93, 197–222, doi:10.1007/s10584-008-9461-6, 2008.

Title Page

Abstract | Introduction

Conclusions | References

Tables | Figures

◄ | ►

◄ | ►

Back | Close

Full Screen / Esc

Printer-friendly Version

Interactive Discussion

R Core Team: R: A Language and Environment for Statistical Computing, Foundation for Statistical Computing, Vienna, Austria, 2012.

Renner, M. and Bernhofer, C.: Long term variability of the annual hydrological regime and sensitivity to temperature phase shifts in Saxony/Germany, Hydrol. Earth Syst. Sci., 15, 1819–1833, doi:10.5194/hess-15-1819-2011, 2011.

Roald, L. A.: Climate Change Impacts on Streamflow in Norway, Norwegian Water Resources and Energy Directorate, Oslo, 2006.

Sælthun, N.: The Nordic HBV model, NVE publication no. 7, Norwegian Water Resources and Energy Diretorate, Oslo, 1996.

Seneviratne, S. I., Nicholls, N., Easterling, D. R., Goodess, C. M., Kanae, S., Kossin, J., Luo, Y., Marengo, J., McInnes, K., Rahimi, N., Reichstein, M., Sorteberg, A., Vera, C., and Zhang, X.: Changes in climate extremes and their impacts on the natural physical environment, in: Managing the Risks of Extreme Events and Disasters to Advance Climate Change Adaptation, edited by: Field, C. B., Barros, V., Stocker, T. F., Qin, D., Dokken, D. J., Ebi, K. L., Mastrandrea, D. M., Mach, K. J., Plattner, G.-K., Allen, S. K., Tignor, M., and Midgley, G. F., Cambridge University Press, Cambridge, UK, and New York, NY, USA, 109–230, 2012.

Stahl, K., Hisdal, H., Hannaford, J., Tallaksen, L. M., van Lanen, H. A. J., Sauquet, E., Demuth, S., Fendekova, M., and Jódar, J.: Streamflow trends in Europe: evidence from a dataset of near-natural catchments, Hydrol. Earth Syst. Sci., 14, 2367–2382, doi:10.5194/hess-14-2367-2010, 2010.

Stewart, I. T., Cayan, D. R., and Dettinger, M. D.: Changes toward earlier streamflow timing across western North America, J. Climate, 18, 1136–1155, doi:10.1175/JCLI3321.1, 2005.

Sunyer, M. A., Madsen, H., Rosbjerg, D., and Arnbjerg-Nielsen, K.: Regional interdependency of precipitation indices across Denmark in two ensembles of high resolution RCMs, J. Climate, 26, 7912–7928, doi:10.1175/JCLI-D-12-00707.1, 2013.

Teutschbein, C. and Seibert, J.: Bias correction of regional climate model simulations for hydrological climate-change impact studies: review and evaluation of different methods, J. Hydrol., 456–457, 12–29, doi:10.1016/j.jhydrol.2012.05.052, 2012.

Tolson, B. A. and Shoemaker, C. A.: Dynamically dimensioned search algorithm for computationally efficient watershed model calibration, Water Resour. Res., 43, W01413, doi:10.1029/2005WR004723, 2007.

Uppala, S. M., Kållberg, P. W., Simmons, A. J., Andrae, U., Bechtold, V. D. C., Fiorino, M., Gibson, J. K., Haseler, J., Hernandez, A., Kelly, G. A., Li, X., Onogi, K., Saarinen, S., Sokka, N., Allan, R. P., Andersson, E., Arpe, K., Balmaseda, M. A., Beljaars, A. C. M., Van De Berg, L., Bidlot, J., Bormann, N., Caires, S., Chevallier, F., Dethof, A., Dragosavac, M., Fisher, M., Fuentes, M., Hagemann, S., Hólm, E., Hoskins, B. J., Isaksen, L., Janssen, P. A. E. M., Jenne, R., Mcnally, A. P., Mahfouf, J.-F., Morcrette, J.-J., Rayner, N. A., Saunders, R. W., Simon, P., Sterl, A., Trenberth, K. E., Untch, A., Vasiljevic, D., Viterbo, P., and Woollen, J.: The ERA-40 re-analysis, Q. J. Roy. Meteorol. Soc., 131, 2961–3012, doi:10.1256/qj.04.176, 2005.

Van der Linden, P. and Mitchell, J. F. B.: ENSEMBLES: Climate Change and its Impacts: Summary of Research and Results from the ENSEMBLES Project, Met Office Hadley Centre, Exeter, UK, 2009.

Van Roosmalen, L., Sonnenborg, T. O., Jensen, K. H., and Christensen, J. H.: Comparison of hydrological simulations of climate change using perturbation of observations and distribution-based scaling, Vadose Zone J., 10, 136, 2011.

Veijalainen, N., Lotsari, E., Alho, P., Vehviläinen, B., and Käyhkö, J.: National scale assessment of climate change impacts on flooding in Finland, J. Hydrol., 391, 333–350, doi:10.1016/j.jhydrol.2010.07.035, 2010.

Vikhamar Schuler, D., Beldring, S., Førland, E. J., Roald, L. A., and Engen-Skaugen, T.: Snow cover and snow water equivalent in Norway?: – Current conditions (1961–1990) and scenarios for the future (2071–2100), met.no report 01/2006, Oslo, 2006.

Wilby, R. L. and Harris, I.: A framework for assessing uncertainties in climate change impacts: low-flow scenarios for the River Thames, UK, Water Resour. Res., 42, W02419, doi:10.1029/2005WR004065, 2006.

Wilson, D., Hisdal, H., and Lawrence, D.: Has streamflow changed in the nordic countries? – Recent trends and comparisons to hydrological projections, J. Hydrol., 394, 334–346, doi:10.1016/j.jhydrol.2010.09.010, 2010.

Title Page

Abstract | Introduction

Conclusions | References

Tables | Figures

◀ | ▶

◀ | ▶

Back | Close

Full Screen / Esc

Printer-friendly Version

Interactive Discussion

Table 1. Characteristics of the six study catchments.

Catchment Property	Krinsvatn	Fustvatn	Øvrevatn	Junkerdalselv	Atnasjø	Kråkfoss
Area (km^2)	207	526	525	420	463	433
Median elevation (m a.s.l.)	349	436	841	835	1205	445
Elevation range (m a.s.l.)	87–629	39–812	145–1636	117–1703	701–2169	105–803
Average annual P (mm)	2291	3788	832	3031	840	2092
Average annual Q (mm)	1992	3017	564	2722	672	1798
Land cover, % lake	8	6	10	0	2	4
Land cover, % glacier	0	< 1	4	1	< 1	0
Land cover, % forest	20	38	23	25	20	76
Land cover, % marsh and bog	9	5	1	1	2	5
Land cover, % sparse vegetation above treeline	57	37	57	63	69	0
Anthropogenic land use (%)	0.4	0.0	0.7	0.5	0.4	11.2

Table 2. The GCM/RCM combinations from ENSEMBLES used for the hydrological projections. The full names of the institute abbreviations are: SMHI – Swedish Meteorological and Hydrological Institute, met.no – the Norwegian Meteorological Institute, KNMI – The Royal Netherlands Meteorological Institute, MPI – Max Planck Institute for Meteorology (Germany), ICTP – International Centre for Theoretical Physics (Italy), METEO-HC – The Met Office Hadley Centre (UK).

Global Climate Model (GCM)	Regional Climate Model (RCM)	Institute
BCM	RCA	SMHI
	HIRHAM	met.no
ECHAM5	RACMO	KNMI
	REMO	MPI
	RegCM	ICTP
HadCM3Q0	HadRM3Q0	METEO-HC
HadCM3Q3	HadRM3Q3	METEO-HC
HadCM3Q16	HadRM3Q16	METEO-HC
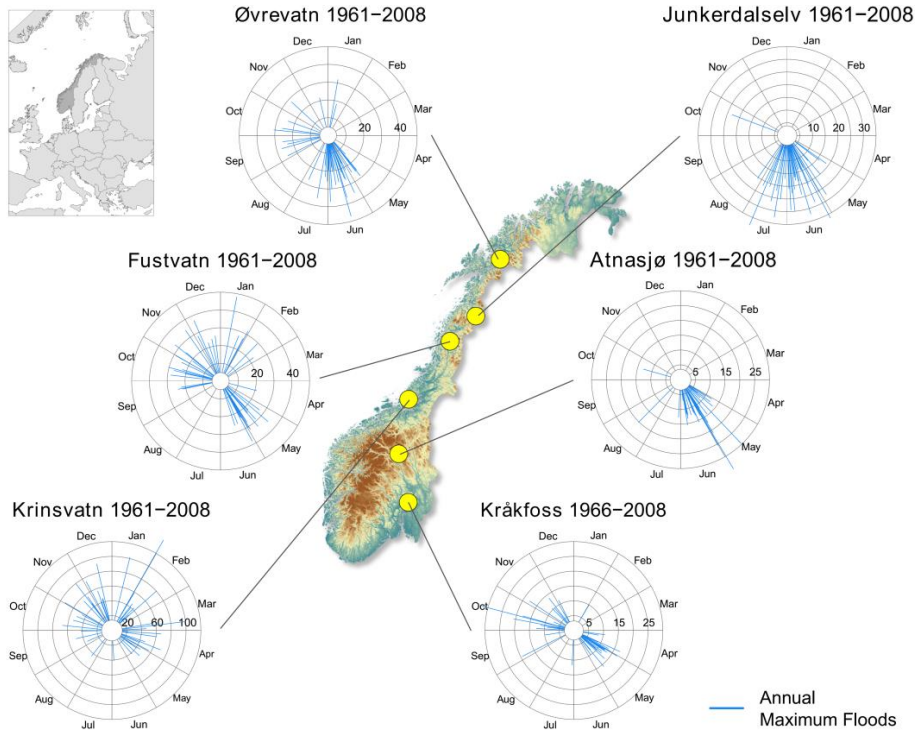
Figure 1. The location of the six study catchments and their current flood regime demonstrated by flood roses indicating the magnitude and timing of observed annual maximum floods. Values are given as specific discharge [mm day^{-1}].

Full Screen / Esc

Figure 2. The distributions of POT events for the reference period from observed (grey) and simulated streamflow series generated by the calibrated HBV model using (from left to right panels): (i) observed climate data with the 25 best-fit parameter sets, (ii) the entire ensemble (i.e. all GCM/RCM combinations, LAMs, and hydrological parameter sets), (iii) the data locally adjusted by EQM, (iv) the data locally-adjusted by XDS, and (v) the raw RCM data. For the simulations (iii)–(v) only one best-fit HBV parameter set is considered.
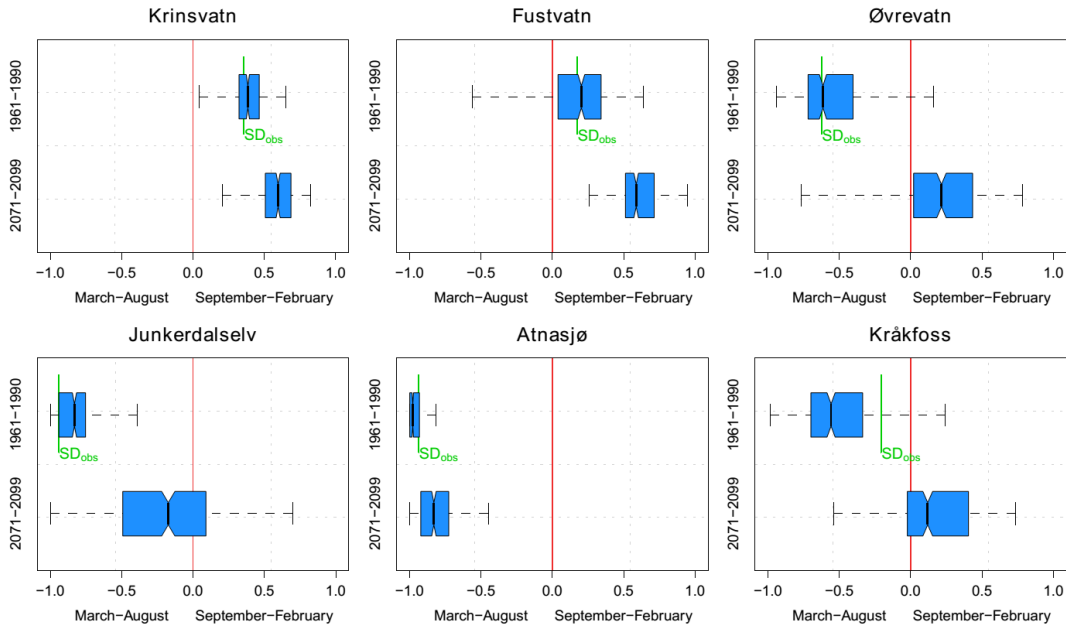
Figure 3. Boxplots showing the seasonality index S_D for all ensemble realizations for the reference and future period. The boxes show the interquartile of the values; the whiskers show the full range of the projections. The green bars in the upper panel of each plot (SD_{obs}) indicate the observed seasonality index S_D.
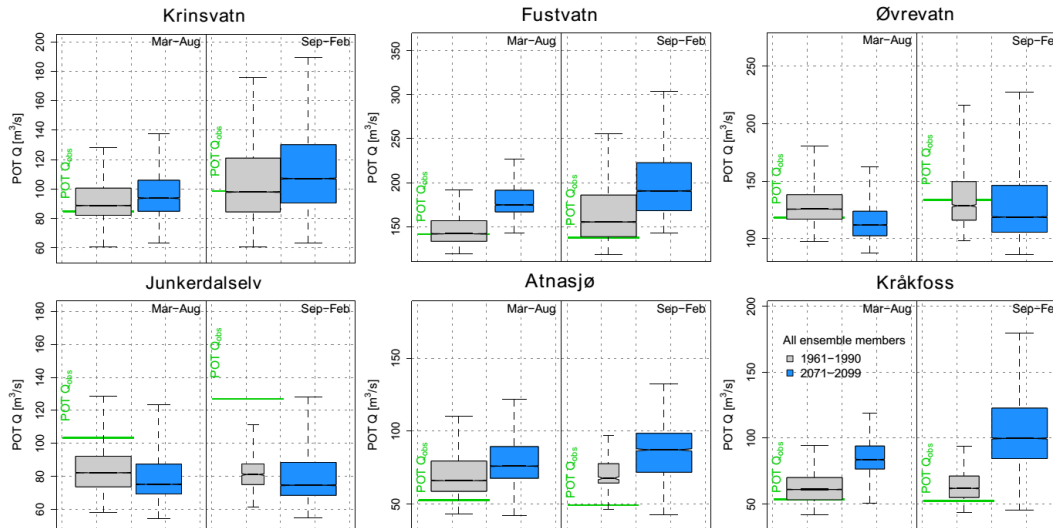
Figure 4. Boxplots showing the median and interquartile magnitudes of the simulated POT events from all ensemble realizations for the reference (grey boxes) and future period (blue boxes), separated with respect to the two basic flood seasons in Norway (spring/summer – left panels; autumn/winter – right panels). The whisker-range corresponds to twice the interquartile range. The green bars (POT$_{obs}$) indicate the mean magnitudes of observed POT events. The width of the boxes indicates the number of events within each group (the widths are proportional to the square-root of the number of events).
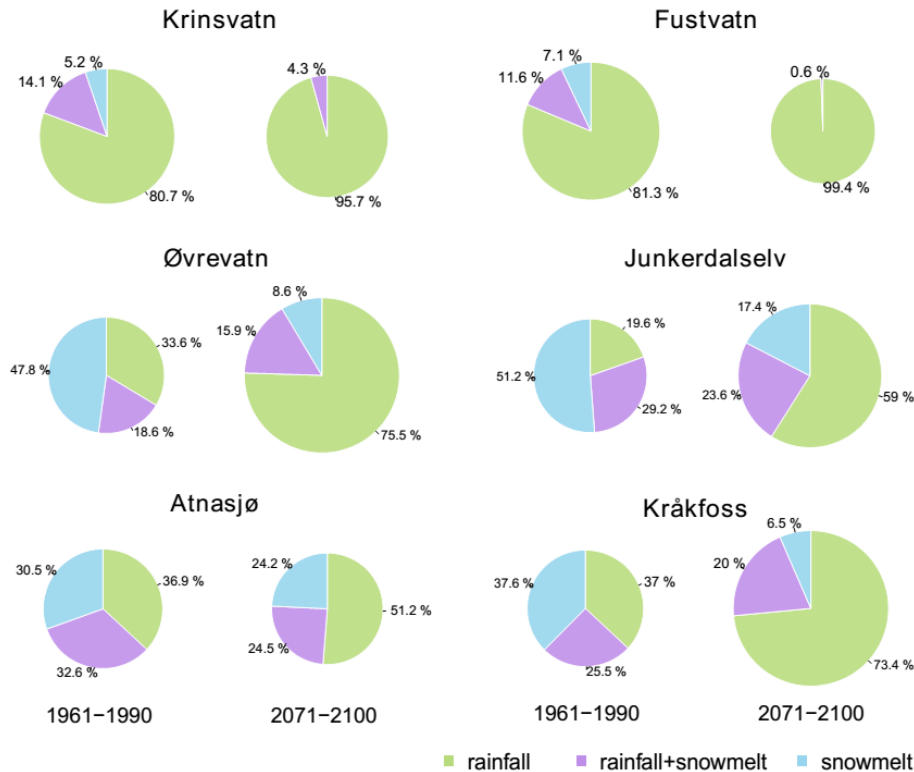
Figure 5. Percentage of POT events according to their FGPs in relation to the total number of events for the reference (left pies) and future period (right pies). The diameter of the pies for the future period indicates the direction of change in the total number of events.
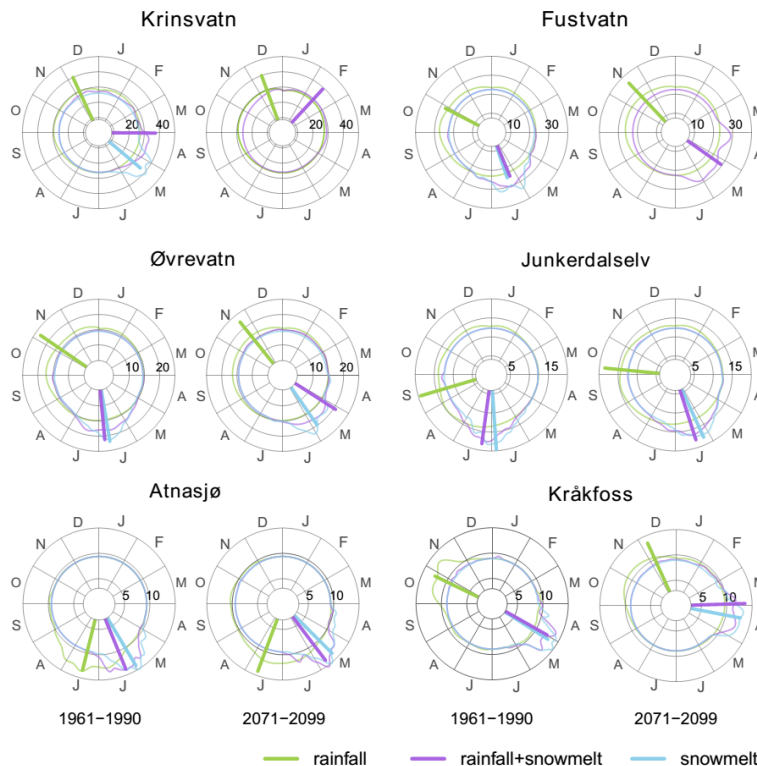
Figure 6. Circular plots showing (i) the circular kernel density function of the simulated POT events according to their FGPs [normalized; no units], and (ii) the median POT event magnitude [mm day^{-1}] as bars according to their circular mean Julian date of occurrence and their FGPs for the reference and future period.

Title Page

Abstract | Introduction

Conclusions | References

Tables | Figures

◀ | ▶

◀ | ▶

Back | Close

Full Screen / Esc

Printer-friendly Version
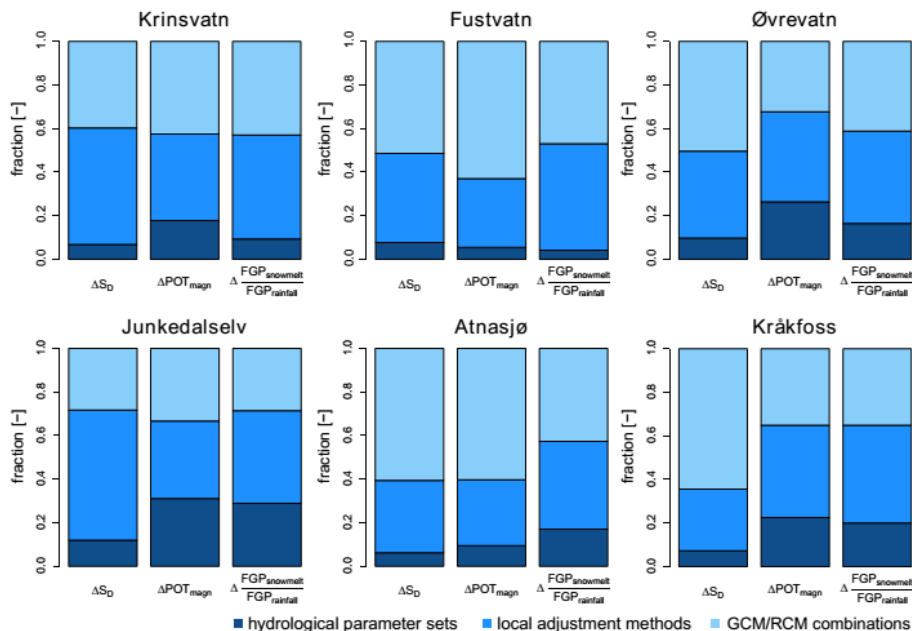
Interactive Discussion

Figure 7. The fractions of total variance [–] as a measure for uncertainty, explained by (i) the GCM/RCM combinations (light blue), (ii) the local adjustment methods (medium blue), and (iii) the hydrological parameterization (dark blue) with respect to three target variables: (1) change in the seasonality index S_D, (2) change in the mean POT event magnitude; (3) change in the ratio of snowmelt and rainfall generated POT events.